PHYSICAL REVIEW B VOLUME 8, NUMBER 5 1 SEPTEMBER 1973

Perturbation Expansion of the Linear Hubbard Model†

D. J. Klein
Department of Physics, The University of Texas at Austin, Austin, Texas 78712

W. A. Seitz*
Department of Chemistry, The University of Texas at Austin, Austin, Texas 78712

(Received 11 December 1972)

A linked-diagram perturbation expansion of the linear half-filled-band Hubbard model is developed and carried out through seventh order. The zero-order Hamiltonian is taken to be the intrasite Coulomb repulsion terms, and the perturbation is taken to be the intersite interaction. The degenerate perturbation theory applied here results in an effective Hamiltonian defined on a simple spin space, and is found to consist of terms involving nearest-neighbor, next-nearest-neighbor, and biquadratic spin operators.

I. INTRODUCTION

The Hubbard Hamiltonian has been employed as a model for the investigation of conditions for ferromagnetism[1,2] and for the metal-insulator transition.[1] More recently the model has been employed in the description[3,4] of the magnetic, electrical, and optical properties of a variety of aromatic donor-acceptor and aromatic free-radical salt crystals. The simplest form of this Hubbard Hamiltonian for a linear chain is

$$H \equiv H^0 + V, \tag{1.1}$$

where

$$H^0 \equiv I \sum_n a^\dagger_{n\alpha} a_{n\alpha} a^\dagger_{n\beta} a_{n\beta} ,$$

$$V \equiv T \sum_n \sum_\sigma (a^\dagger_{n\sigma} a_{n+1\sigma} + a^\dagger_{n+1\sigma} a_{n\sigma}) . \tag{1.2}$$

Here $a^\dagger_{n\sigma}$ and $a_{n\sigma}$ are fermion creation and annihilation operators for an electron of spin σ on site n. The parameters I and T may be identified as intrasite Coulomb repulsion and intersite charge-transfer integrals. Although this Hamiltonian is quite simple in appearance, accurate solution for the thermodynamic properties has proved difficult.

In the organic crystals referred to in Refs. 3 and 4, the aromatic molecules are planar and form linear stacks. Since the intrastack-charge-transfer matrix elements are much larger than interstack ones, a one-dimensional treatment is in order. A number of different cases arise. For free-radical salts each site may have a single unpaired electron and the half-filled-band (i.e., "valence" electrons and sites equal in number) Hubbard model applies. For the case of sufficiently strong donors and acceptors the ground state may primarily consist of alternating donor cations and acceptor anions; in this case the half-filled-band Hubbard model also applies, although an "orbital energy" alternating down the chain should be introduced. In other cases, not of interest here, partially filled Hubbard models apply. Further, evidence indicates[3,4] that the magnitude of the charge transfer interaction T is typically a small fraction ($\sim \frac{1}{6}$) of the Coulomb repulsion I.

Here we consider a perturbation expansion for the linear-chain Hubbard model with the same number of electrons as sites. We treat the intrasite repulsions of H^0 as the zero-order Hamiltonian and the electron-hopping term V as the perturbation, so that the expansion applies in the case $|T| \ll I$. The zero-order ground state with one electron per site has a high permutational degeneracy. For small intersite interactions T and low temperature (as compared to I) we then expect low-lying states arising from the zero-order ground-state eigenspace to describe accurately the thermodynamic properties. Thus we apply degenerate perturbation theory to only those states arising from this ground-state separated-atom limit. This perturbation formulation should be adequate for the description of molecular crystals referred to above, though it will apparently give information only on the insulator side of any metal-insulator transition. Further, this perturbation expansion does not provide conditions for ferromagnetism, since as seen below it always predicts exchange interactions of antiferromagnetic sign in its region of applicability.

Here we employ a perturbation expansion which is described by des Cloizeaux[5] and Klein[6] and which is equivalent to those described by Buleavski[7] and Primas.[8] The perturbed eigenvalues are to be obtained through the diagonalization of an effective Hamiltonian defined on the zero-order eigenspace. Expansion of this effective Hamiltonian through a given order and truncation yields, after diagonalization, eigenvalues accurate through the given order. Through second order this effective Hamiltonian is of the form of the Heisenberg spin Hamiltonian with nearest-neighbor interactions, as is evident from Anderson's superexchange derivation.[9]

Through fourth order this effective Hamiltonian is of the form of a Heisenberg spin Hamiltonian with nearest- and next-nearest-neighbor interactions.[7] Here we develop the perturbation-expansion techniques and carry out the expansion through sixth order where a Heisenberg spin Hamiltonian with nearest- and next-nearest-neighbor interactions along with three types of biquadratic spin interactions is obtained.

The perturbation expansion of the Hubbard Hamiltonian thus provides a model treatment of weakly interacting sites and the derivation of a Heisenberg spin Hamiltonian. A variety of techniques applicable to spin Hamiltonians can hence be applied in approximating the thermodynamic properties of the Hubbard Hamiltonian at low temperatures and small intersite interaction. In particular, numerical solutions may be carried out on longer finite chains since the dimension of the spin Hamiltonian space is much less than the dimension of the full Hubbard space. Thus it is anticipated that finite chain calculations on Hubbard models which have been carried out[10] for cyclic chains of six and fewer sites may be extended to chains of up to 12 sites via the perturbation expansion given here. Although[10] "it is not easy to unambiguously extrapolate these results for finite systems [of six and fewer sites] to the infinite system," the calculations of Bonner and Fisher[11] indicate that results for chains of 12 and fewer sites should be quite adequate to make useful extrapolations. We then expect such an extrapolated perturbation technique to yield reliable results for small T/I at temperatures much less than I. Indeed such a perturbative treatment may yield more reliable results than a number of other[12-14] approximate many-body techniques. Finally we note that while there are exact results[15] available, they apply primarily to zero-temperature properties (and hence, may be employed as a partial judge of various approximate treatments).

Section II presents the perturbation theory and develops the formal expansion through seventh order. Section III presents a diagrammatic representation of the terms in the expansion which greatly simplifies the tedious substitution processes. Section IV then employs the diagrammatic representation to evaluate the expansion. Appendices A–C outline intermediate steps, prove several theorems about diagrams and evaluate the diagrams in terms of the more usual spin and permutation operators on ordinary spin space. Finally, Sec. V discusses the results and indicates the extension of the present techniques to more general Hamiltonians.

II. PERTURBATION THEORY

We first consider the general perturbation formalism. We define $\mathcal{P}^0$ to be the idempotent and Hermitian projection operator onto the zero-order eigenspace with eigenvalue E^0,

$$H^0\mathcal{P}^0=\mathcal{P}^0H^0=E^0\mathcal{P}^0 . \tag{2.1}$$

As the perturbation V is gradually turned on these zero-order eigenkets evolve. We let $\mathcal{P}$ be the idempotent and Hermitian projection operator onto the space spanned by the perturbed eigenkets which evolved from the zero-order eigenspace. Then assuming every perturbed eigenket has nonzero overlap with the zero-order eigenspace from which it evolved, we may express the perturbed eigenkets of interest in the form $\mathcal{P}|E\rangle$, where $|E\rangle$ is contained in the zero-order eigenspace and E is the perturbed eigenvalue. We have

$$H\mathcal{P}|E\rangle=E\mathcal{P}|E\rangle \tag{2.2}$$

and

$$\mathcal{P}^0H\mathcal{P}\mathcal{P}^0\,|E\rangle=E\mathcal{P}^0\mathcal{P}\mathcal{P}^0\,|E\rangle . \tag{2.3}$$

According to Kato[16] the nth-order term in the expansion of $\mathcal{P}^0\mathcal{P}\mathcal{P}^0$ is

$$(\mathcal{P}^0\mathcal{P}\mathcal{P}^0)^{(n)}=-\sum_{k(n-1)}^{(n)}(k_1,k_2,\ldots,k_{n-1}) \tag{2.4}$$

and the nth-order term of $\mathcal{P}^0(H-E^0)\mathcal{P}\mathcal{P}^0$ is

$$[\mathcal{P}^0(H-E^0)\mathcal{P}\mathcal{P}^0]^{(n)}=\sum_{k(n-1)}^{(n-1)}(k_1,k_2,\ldots,k_{n-1}) . \tag{2.5}$$

Here we have defined

$$(k_1,k_2,\ldots,k_{n-1})\equiv\mathcal{P}^0VS^{(k_1)}VS^{(k_2)}V\cdots VS^{(k_{n-1})}V\mathcal{P}^0, \tag{2.6}$$

$$S^{(k)}\equiv\begin{cases}-\mathcal{P}^0\ , & k=0\\ \left(\dfrac{1-\mathcal{P}^0}{E^0-H^0}\right)^k\ , & k\geq 1\end{cases} \tag{2.7}$$

and $\sum_{k(m)}^{(n)}$ denotes a sum over all sequences of nonnegative indices $k_1, k_2, \ldots, k_m$ which sum to n.

Kato's expansion yields an effective Hamiltonian $\mathcal{P}^0(H-E^0)\mathcal{P}\mathcal{P}^0$ with a nonidentity effective overlap $\mathcal{P}^0\mathcal{P}\mathcal{P}^0$. Also, truncation of these effective operators at a given order sometimes yields a problem in which the wrong N-dependence of the eigenvalues is obtained. These problems are avoided if we eliminate the effective overlap operator, as described by Löwdin,[17] to give a new effective Hamiltonian problem

$$\mathcal{H}\,|E'\rangle=(E-E^0)\,|E'\rangle , \tag{2.8}$$

where $|E'\rangle=(\mathcal{P}^0\mathcal{P}\mathcal{P}^0)^{1/2}\,|E\rangle$ and

$$\mathcal{H}\equiv\frac{1}{(\mathcal{P}^0\mathcal{P}\mathcal{P}^0)^{1/2}}\,\mathcal{P}^0(H-E^0)\mathcal{P}\mathcal{P}^0\,\frac{1}{(\mathcal{P}^0\mathcal{P}\mathcal{P}^0)^{1/2}} . \tag{2.9}$$

The nth-order term in the perturbation expansion of $1/(\mathcal{P}^0\mathcal{P}\mathcal{P}^0)^{1/2}$ is

$$\left(\frac{1}{(\mathcal{P}^0\mathcal{P}\mathcal{P}^0)^{1/2}}\right)^{(n)} = \sum_{j=1}^{n} \frac{(-1)^j}{2^{2j}} \sum_{m(j)}^{(n-j)} (\mathcal{P}^0\mathcal{P}\mathcal{P}^0)^{(m_1+1)}$$

$$\times(\mathcal{P}^0\mathcal{P}\mathcal{P}^0)^{(m_2+1)} \cdots (\mathcal{P}^0\mathcal{P}\mathcal{P}^0)^{(m_j+1)} . \quad (2.10)$$

Substitution of the terms (2.4) into (2.10) followed by substitution of the terms (2.5) and (2.10) into (2.9) yields the terms of the formal perturbation expansion of the effective Hamiltonian $\mathcal{H}$.

For the Hubbard model the zero-order Coulomb repulsion interaction H^0 of (1.2) has eigenvalues mI, where m is the number of doubly occupied sites. Hence, the ground state has energy $E^0 = 0$ corresponding to single occupancy of every site. The perturbation V connects ground-state configurations only to states with one double occupancy (and one vacancy); these ionic states are not in the zero-order ground-state eigenspace, so that

$$\mathcal{P}^0 V \mathcal{P}^0 = 0 . \quad (2.11)$$

Similarly, the application of such charge transfer interactions to any zero-order ground-state ket any odd number of times will not return it to the $\mathcal{P}^0$ eigenspace. Hence,

$$(k_1, k_2, \ldots, k_n) = 0, \quad n \text{ even} \quad (2.12)$$

$$(k_1, k_2, \ldots, k_m, 0, l_1, l_2 \ldots, l_n) = 0, \quad m \text{ or } n \text{ even}. \quad (2.13)$$

We also readily see that

$$(k_1, \ldots, k_m)(l_1, \ldots, l_n) = -(k_1, \ldots, k_m, 0, l_1, \ldots, l_n). \quad (2.14)$$

Also recalling that $E^0 = 0$ and that the lowest ionic states have energy I, we obtain

$$(k_1, k_2, \ldots, k_n) = (-1/I)^{k_1-1}(1, k_2, \ldots, k_n) = (-1/I)^{k_n-1}(k_1, k_2, \ldots, k_{n-1}, 1). \quad (2.15)$$

Since the mth-order term $\mathcal{H}^{(m)}$ in the expansion of $\mathcal{H}$ involves an odd number of V operators when m is odd, the results in (2.12)–(2.14) imply that

$$\mathcal{H}^{(2n+1)} = 0 . \quad (2.16)$$

Using (2.12)–(2.16) for the Hubbard model, we evaluate the expression for even orders,

$$\mathcal{H}^{(0)} = 0, \quad \mathcal{H}^{(2)} = (1) ,$$

$$\mathcal{H}^{(4)} = (1, 1, 1) - (1/I)(1, 0, 1) ,$$

$$\mathcal{H}^{(6)} = (1, 1, 1, 1, 1) + \tfrac{1}{2}(1, 2, 1, 0, 1) + \tfrac{1}{2}(1, 0, 1, 2, 1) - (3/2I)(1, 1, 1, 0, 1) - (3/2I)(1, 0, 1, 1, 1) + (2/I^2)(1, 0, 1, 0, 1) . \quad (2.17)$$

The final result is obtained on substituting (1.2) and (2.7) into (2.6), (2.6) into (2.17), and then converting the products of creation and annihilation operators into spin operators and then permutation operators using the results of Appendix A. To aid in this complex substitution process we first introduce some additional concepts.

III. X OPERATORS, DIAGRAMS, AND THE LINKED EXPANSION

We define

$$X_{ij} \equiv \sum_{\sigma} a_{i\sigma}^{\dagger} a_{j\sigma} , \quad (3.1)$$

which transfers an electron from site j to i (or gives zero). The fermion anticommutation relations yield

$$[X_{ij}, X_{kl}] = \delta_{jk} X_{il} - \delta_{il} X_{kj} \quad (3.2)$$

and these X operators are[18] the basis elements of the Lie algebra of the unitary group $\mathfrak{U}(N)$. Since the zero-order Hamiltonian and perturbation can be expressed as

$$V = T \sum_{n} (X_{nn+1} + X_{n+1n}) ,$$
$$H^0 = \tfrac{1}{2} I \sum_{n} (X_{nn}^2 - X_{nn}) , \quad (3.3)$$

the perturbation formalism can also be developed entirely in terms of these X operators. We further represent an X_{ij} by an *arrow* directed from site j to site i, as in Fig. 1.

A product of X operators may then be represented by a *labeled diagram* consisting of the arrows for the individual X operators ordered such that if X_{ij} is to the left of X_{kl} in the product then the first arrow is located above the second in the diagram. An *unlabeled diagram* consists of a sum of labeled diagrams all translationally equivalent, and is depicted by removing the labels from any one of the labeled diagrams in the sum. Further, enclosing a set of arrows in a diagram in anticommutator brackets indicates a sum over all possible orderings of the enclosed arrows. Several diagrams are found in Appendix A, where they are evaluated in terms of spin and permutation operators. In Appendix B they are further related to double cosets of the symmetric group, and a second method of evaluating them is described.

We define a product $X_{i_1 j_1} X_{i_2 j_2} \cdots X_{i_n j_n}$ of X operators and its corresponding diagram to be *linked* if and only if the integers $i_1, j_1, i_2, j_2, \ldots, i_n, j_n$ cannot be divided into two or more disjoint sets with each pair i_k, j_k in the same set. We also write

FIG. 1. One-arrow diagram.

$$\mathfrak{L}(X_{i_1 j_1}\cdots X_{i_n j_n}) \equiv \begin{cases} X_{i_1 j_1}\cdots X_{i_n j_n}, & \text{linked} \\ 0, & \text{unlinked}. \end{cases} \tag{3.4}$$

It may be shown[6] that the present perturbation expansion of the effective Hamiltonian consists only of linked terms, by which we mean that on substituting V as in (3.3) into the expressions for $\mathcal{K}^{(n)}$ only linked n-fold products of X operators occur, before any commutation or other manipulation takes place. Alternatively we may describe all the unlinked terms as canceling. We hence rewrite Eqs. (2.17) as

$$\begin{aligned} &\mathcal{K}^{(2)} = \mathfrak{L}(1), \quad \mathcal{K}^{(4)} = \mathfrak{L}(1,1,1) - (1/I)\,\mathfrak{L}(1,0,1), \\ &\mathcal{K}^{(6)} = \mathfrak{L}(1,1,1,1,1) + \tfrac{1}{2}\mathfrak{L}(1,2,1,0,1) \\ &\quad + \tfrac{1}{2}\mathfrak{L}(1,0,1,2,1) - (3/2I)\,\mathfrak{L}(1,1,1,0,1) \\ &\quad - (3/2I)\,\mathfrak{L}(1,0,1,1,1) + (2/I^2)\,\mathfrak{L}(1,0,1,0,1). \end{aligned} \tag{3.5}$$

It is the canceling of the unlinked terms which assures that the present perturbation expansion yields the correct N dependence of the eigenvalues computed from a truncated expansion of the effective Hamiltonian.

Since $\mathcal{P}^0$ is applied to both the left and right of each term in the perturbation expansion, the total number of arrows coming into any site must be the same as the number leaving. Hence, defining a *cyclic* diagram to consist of a product of X operators $X_{i_1 i_2}$, $X_{i_2 i_3}$, ..., $X_{i_n i_1}$ in any order, we see that the perturbation is, in fact, composed of (linked) cyclic diagrams. In the following we will assume that the application of $\mathcal{P}^0$ before and after each cycle is understood, so that it will not be written down explicitly.

IV. EVALUATION OF THE PERTURBATION EXPANSION

In this section we find that the effective Hamiltonian through seventh order may be expressed as linear combinations of the permutation operators on spin space,

$$\begin{aligned} A_1 &\equiv \sum_n [1 - (n, n+1)], \\ A_2 &\equiv \sum_n [1 - (n, n+2)], \\ A_3 &\equiv \sum_n [1 - (n, n+3)], \\ B_1 &\equiv \sum_n [1 - (n, n+1)(n+2, n+3)], \\ B_2 &\equiv \sum_n [1 - (n, n+2)(n+1, n+3)], \\ B_3 &\equiv \sum_n [1 - (n, n+3)(n+1, n+2)]. \end{aligned} \tag{4.1}$$

We first evaluate the second-order term in the expansion of $\mathcal{K}$,

$$\begin{aligned} \mathcal{K}^{(2)} &= \mathfrak{L}(1) \\ &= \mathfrak{L}\left(\mathcal{P}^0 V \frac{1-\mathcal{P}^0}{E^0 - H^0} V \mathcal{P}^0\right) = -\frac{1}{I}\,\mathfrak{L}(\mathcal{P}^0 V V \mathcal{P}^0). \end{aligned} \tag{4.2}$$

Here we have used (2.6) and (2.7) and the fact that V connects ground-state kets only to kets of zero-order energy I. Using the diagrammatic notation of Sec. III we find $\mathfrak{L}(1)$ is $-2T^2/I$ times the first of the two-arrow diagrams in Fig. 2. Equation (A6) then gives us

$$\mathcal{K}^{(2)} = -(2T^2/I)A_1. \tag{4.3}$$

This result agrees with Anderson[9] and Buleavski.[7]

We next turn to the evaluation of the fourth-order term. Using the linked diagrammatic expansion, we see $\mathfrak{L}(1,1,1)$ is given as T^4/I^3 times the diagrams of Fig. 3, where theorem A.2 is used. Similarly, using theorem A.3, $\mathfrak{L}(1,0,1)$ is given as $-T^4/I^2$ times the diagrams of Fig. 4. Evaluation of these diagrams is carried out in Appendix C to yield

$$\begin{aligned} \mathcal{K}^{(4)} &= \mathfrak{L}(1,1,1) - (1/I)\mathfrak{L}(1,0,1) \\ &= (8T^4/I^3)A_1 - (2T^4/I^3)A_2. \end{aligned} \tag{4.4}$$

This result agrees with Buleavski.[7]

Evaluation of the sixth-order term employs the same methods, though the number of diagrams is greatly increased. For the (1,1,1,1,1) term of $\mathcal{K}^{(6)}$ we classify the possible "excitation paths" according to the number of doubly occupied sites after each application of V. This classification is given in Table I, where the factors listed there are simply the appropriate coefficients multiplying the corresponding diagrams. We find that diagrams of types c, e, g, h, and i as given in Table I have no linked contribution. Hence,

$$\begin{aligned} &\mathfrak{L}(1,1,1,1,1) \\ &\quad = -(T^6/I^5)\,\mathfrak{L}(\text{type } a) - (T^6/2I^5)\,\mathfrak{L}(\text{type } b) \\ &\quad\quad - (T^6/2I^5)\,\mathfrak{L}(\text{type } d) - (T^6/4I^5)\,\mathfrak{L}(\text{type } f). \end{aligned} \tag{4.5}$$

The linked portions of the diagrams of types a, b, and f are given in Fig. 5. We also note that diagrams of type d are Hermitian conjugates of those of type b. The evaluation of these different diagrams is outlined in Appendix C. The result is

$$\mathfrak{L}(1,1,1,1,1) = -(T^6/I^5)\{140A_1 - 36A_2 + 12A_3$$

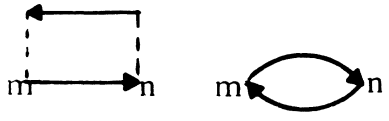

FIG. 2. Two-arrow diagrams.

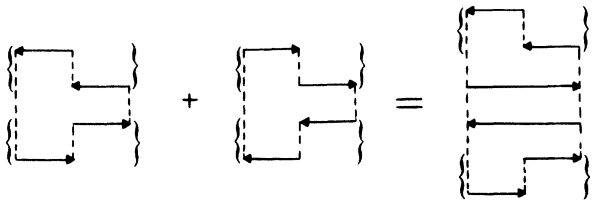

FIG. 3. Diagrams appearing in the expansion of $\mathfrak{L}(1, 1, 1)$, and an application of theorem A. 2.

$$-42B_1+10B_2-10B_3\}. \quad (4.6)$$

In Fig. 6 we present the diagrammatic representation of the linked portion of (1, 0, 1, 1, 1). Again using the results of Appendix C gives

$$\mathfrak{L}(1,0,1,1,1)+\mathfrak{L}(1,1,1,0,1)$$
$$=-(T^6/I^4)\{232A_1-80A_2+24A_3$$
$$-48B_1+16B_2-16B_3\}, \quad (4.7)$$

where we have noted that (1, 0, 1, 1, 1) and (1, 1, 1, 0, 1) are Hermitian conjugates. The linked portions of (1, 0, 1, 2, 1) and (1, 2, 1, 0, 1) may be treated very similarly, since the diagrammatic representation is as given in Fig. 6 except that the coefficient of the fifth diagram is $\frac{1}{4}$ instead of $\frac{1}{2}$. We obtain

$$\mathfrak{L}(1,0,1,2,1)+\mathfrak{L}(1,2,1,0,1)$$
$$=(T^6/I^5)\{208A_1-64A_2+16A_3-40B_1+8B_2-8B_3\}. \quad (4.8)$$

Finally, again using the method of Appendix C, we obtain

$$\mathfrak{L}(1,0,1,0,1)=-(T^6/I^3)\{176A_1-64A_2+16A_3$$
$$-24B_1+8B_2-8B_3\}, \quad (4.9)$$

where the diagrammatic representation is given in Fig. 7. Substitution of (4. 5) and (4. 9) into (3. 5) gives

TABLE I. Excitation paths in (1, 1, 1, 1, 1).

Type	Number of applications of perturbation 1	2	3	4	5	Factor
a	1	1	1	1	1	$-1(T^6/I^5)$
b	1	1	1	2	1	$-\frac{1}{2}(T^6/I^5)$
c	1	1	2	1	1	$-\frac{1}{2}(T^6/I^5)$
d	1	2	1	1	1	$-\frac{1}{2}(T^6/I^5)$
e	1	1	2	2	1	$-\frac{1}{4}(T^6/I^5)$
f	1	2	1	2	1	$-\frac{1}{4}(T^6/I^5)$
g	1	2	2	1	1	$-\frac{1}{4}(T^6/I^5)$
h	1	2	2	2	1	$-\frac{1}{8}(T^6/I^5)$
i	1	2	3	2	1	$-\frac{1}{12}(T^6/I^5)$

$$\mathfrak{K}^{(6)}=-(T^6/I^5)\{40A_1-12A_2+2B_1-2B_2+2B_3\}. \quad (4.10)$$

We note that the coefficient of A_3 is zero in $\mathfrak{K}^{(6)}$.

V. DISCUSSION AND CONCLUSION

Collecting (4. 3), (4. 4), and (4. 10) together yields the expansion of $\mathfrak{K}$ accurate through seventh order:

$$\mathfrak{K}=\{-2(T/I)^2+8(T/I)^4-40(T/I)^6\}IA_1$$
$$+\{-2(T/I)^4+12(T/I)^6\}IA_2-2(T/I)^6I(B_1-B_2+B_3)$$
$$+\text{eighth order and higher.} \quad (5.1)$$

The expansion is expected to yield accurate results for the low-lying states for sufficiently small T/I. The result is a spin Hamiltonian containing first- and second-nearest-neighbor terms in addition to some small biquadratic terms.

The systematized methods of determining the expansion as described here have simplified the computation. The various theorems of the appendices

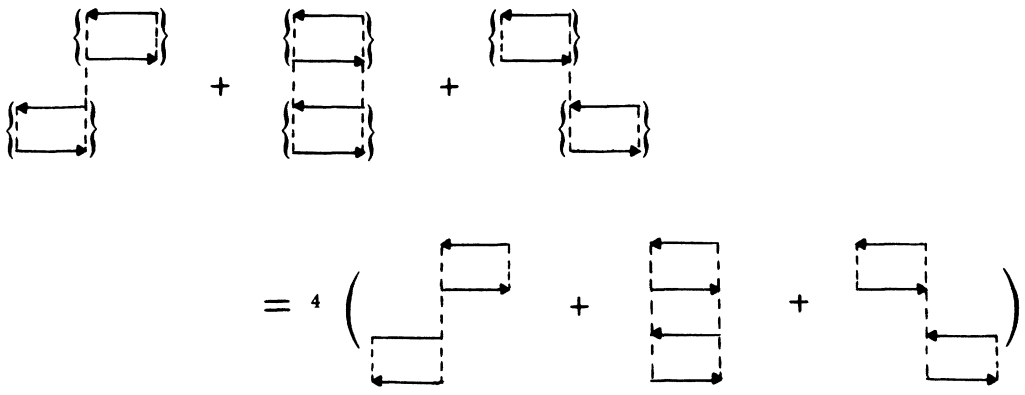

FIG. 4. Diagrams appearing in the expansion of $\mathfrak{L}(1, 0, 1)$.

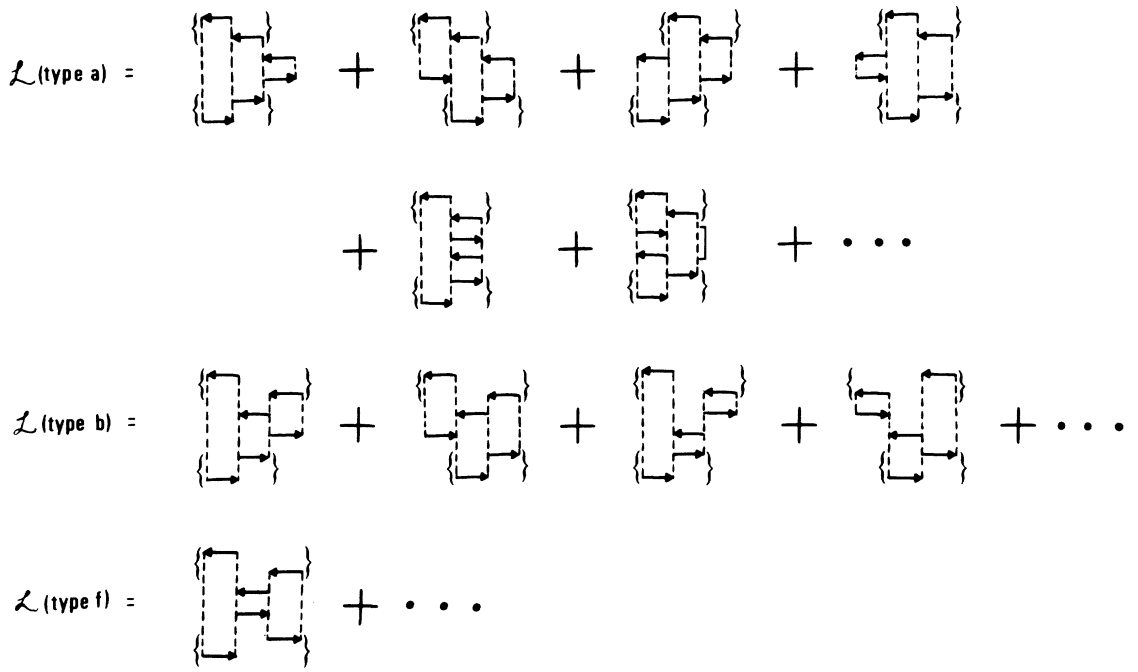

FIG. 5. Different types of linked diagrams occurring in (1, 1, 1, 1, 1). The extra diagrams not listed are merely arrow reversals related to those already listed. There is one arrow reversal for each diagram listed except for the third and fourth diagrams of type b, for which there are three.

provide different approaches to evaluating diagrams so as to make some internal checks. That the unlinked terms cancel was also verified by computation.

The methods are evidently applicable to higher-dimensional Hubbard Hamiltonians, modified Hubbard Hamiltonians, and yet other more general Hamiltonians. It is to be expected that such techniques should be of use in the derivation of Heisenberg spin Hamiltonians. Systematic treatment of the higher-order terms in such expansions, as is emphasized here, should often be of interest. In such more complex situations it is of importance to distinguish intersite interactions between different pairs of sites, since a term of a low order in an interaction between two distant sites may be much less important than a term of high order in an interaction between two neighboring sites. We could treat this formally by introducing different dummy perturbation parameters for interactions between different pairs of sites. For instance, for a term in the Hamiltonian associated with the qth double coset (see Appendix B and Refs. 19–21) and the double coset symbol D^q with (m,n)th elements D^q_{mn}, we would identify the perturbation order $\Pi_{m\neq n}\lambda_{mn}^{D^q_{mn}}$, where λ_{mn} is the dum-

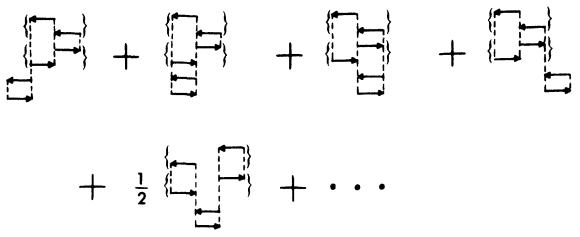

FIG. 6. Linked diagrams occurring in (1, 0, 1, 1, 1). The unlisted portion includes three arrow reversals for each of the listed diagrams.

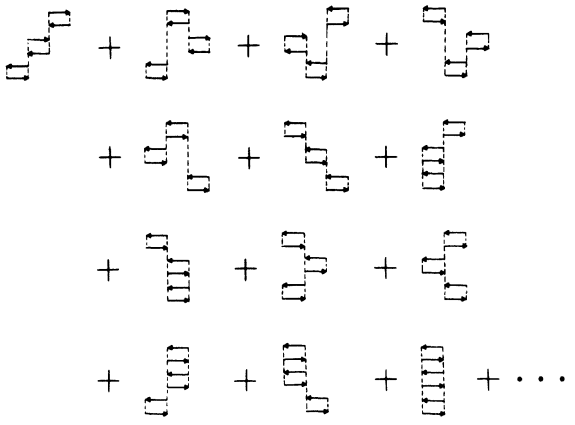

FIG. 7. Linked diagrams occurring in (1, 0, 1, 0, 1). The unlisted portion includes seven arrow reversals for each of the listed diagrams.

my perturbation parameter for interactions between sites m and n. Further, one may treat cases with a nonidentity overlap in a similar formulation.[6]

As an example of a more complex situation, we briefly discuss Anderson's treatment[9] of superexchange. Anderson argues that the primary contributions to the effective exchange interaction between two paramagnetic sites, m and p, arises from terms we could describe by diagrams as in Fig. 2.

These diagrams are associated with the kinetic and direct exchange terms. Clearly, however, we may imagine a wide variety of additional diagrams which may be important, if we explicitly introduce the diamagnetic site (or sites) which is a mutual neighbor to both m and p. A few such diagrams are displayed in Fig. 8. Some portions of these diagrams of Fig. 8 are implicit in Anderson's treatment, since the zero-order site kets employed are not those constructed by merely orthogonalizing noninteracting site kets, but already include the effect of some intersite interactions such as the crystal-field interactions.

Finally, we again point out that the Heisenberg spin Hamiltonian may be somewhat more easily solved to within a desired degree of accuracy than the corresponding full Hubbard Hamiltonian from which it was derived. Some tests of this likelihood, including computations on finite chains, will be reported in the future.

APPENDIX A: PRIMARY RELATIONS

In this appendix we list some relations among creation and annihilation operators, spin operators, and permutations. Most of these are well known, though a few involving some higher permutations are less familiar. We shall also evaluate some simple diagrams and prove several useful theorems concerning the diagrams.

The relations between fermion and spin operators are

$$S_n^+ = a_{n\alpha}^\dagger a_{n\beta} ,$$

$$\begin{aligned} S_n^- &= a_{n\beta}^\dagger a_{n\alpha} , \\ S_n^z &= \tfrac{1}{2}(a_{n\alpha}^\dagger a_{n\alpha} - a_{n\beta}^\dagger a_{n\beta}) \\ &\approx a_{n\alpha}^\dagger a_{n\alpha} - \tfrac{1}{2} \\ &\approx \tfrac{1}{2} - a_{n\beta}^\dagger a_{n\beta} , \end{aligned} \tag{A1}$$

where the last two lines hold if there is only one electron on site n. We also have relations between spin operators and permutations on spin space,

$$\begin{aligned} (mn) &\approx 2\vec{S}_m \cdot \vec{S}_n + \tfrac{1}{2} \\ (mnp) &\approx \vec{S}_m \cdot \vec{S}_n + \vec{S}_n \cdot \vec{S}_p + \vec{S}_m \cdot \vec{S}_p - 2i\vec{S}_m \cdot \vec{S}_n \times \vec{S}_p + \tfrac{1}{4} . \end{aligned} \tag{A2}$$

Further, since the permutational symmetries of spin space are limited to two-rowed Young diagrams, we find linear dependence among permutations

$$\begin{aligned} (mnp) + (mpn) &\approx (mn) + (np) + (pm) - 1, \\ (mnpq) + (mqpn) &\approx (mn)\,(pq) - (mp)\,(nq) \\ &\quad + (mq)\,(np) + (mp) + (nq) - 1 . \end{aligned} \tag{A3}$$

These relations (A1)–(A3) allow one to start from the definition (1.2) of the perturbation V and eventually deduce the form of the $\mathcal{H}^{(n)}$, for $n \leq 7$.

We now indicate the evaluation of a couple of simple diagrams. First we find that the first two-arrow diagram of Fig. 2 is equal to

$$\begin{aligned} X_{mn}X_{nm} &= a_{m\alpha}^\dagger a_{n\alpha} a_{n\alpha}^\dagger a_{m\alpha} + a_{m\alpha}^\dagger a_{n\alpha} a_{n\beta}^\dagger a_{m\beta} \\ &\quad + a_{m\beta}^\dagger a_{n\beta} a_{n\alpha}^\dagger a_{m\alpha} + a_{m\beta}^\dagger a_{n\beta} a_{n\beta}^\dagger a_{m\beta} \\ &= a_{m\alpha}^\dagger a_{m\alpha}(1 - a_{n\alpha}^\dagger a_{n\alpha}) - a_{m\alpha}^\dagger a_{m\beta} a_{n\beta}^\dagger a_{n\alpha} \\ &\quad - a_{m\beta}^\dagger a_{m\alpha} a_{n\alpha}^\dagger a_{n\beta} + a_{m\beta}^\dagger a_{m\beta}(1 - a_{n\beta}^\dagger a_{n\beta}) \\ &= (\tfrac{1}{2} + S_m^z)(\tfrac{1}{2} - S_n^z) - S_m^+ S_n^- - S_m^- S_n^+ + (\tfrac{1}{2} - S_m^z)(\tfrac{1}{2} - S_n^z) \\ &= \tfrac{1}{2} - 2\vec{S}_m \cdot \vec{S}_n \\ &= 1 - (mn) . \end{aligned} \tag{A4}$$

Similarly, although somewhat more tediously, we find that the three-arrow diagrams of Fig. 9 are equal to

$$(\text{Fig. } 9) = (np) - (mpn) . \tag{A5}$$

To evaluate more complicated diagrams one could continue with the type of procedure outlined in (A4), although considerable effort can be saved through the use of some general theorems concerning the diagrams.

Theorem A.1. Simultaneously turning a diagram upside down and reversing its arrows yields the Hermitian conjugate of the original diagram.

Proof. The proof is immediate on considering the corresponding X-operator products and noting $X_{mn}^\dagger = X_{nm}$.

Theorem A.2. Let wiggly arrows from m to n and n to m represent any two systems of linked

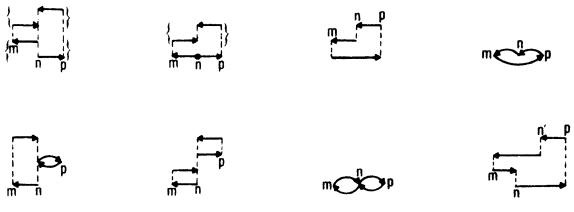

FIG. 8. A few of the many possible diagrams which could contribute to the effective exchange interaction between two paramagnetic sites m and p. Separated by diamagnetic sites n and n'.

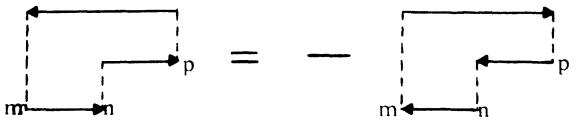

FIG. 9. Three-arrow diagrams.

arrows from sites m to n and n to m. Then the equality of Fig. 10 holds.

Proof. We write the original diagram D as a product of two operators

$$D = P_{mn} P_{nm} ,$$

where P_{mn} and P_{nm} consist of the X-operator products corresponding to the wiggly arrows from sites n to m and sites m to n. After application of P_{nm} site m is vacant and site n is doubly occupied, so that

$$D = P_{mn} \tfrac{1}{2} \sum_{\sigma} (a_{m\sigma} a^{\dagger}_{m\sigma} a^{\dagger}_{n\sigma} a_{n\sigma} + a_{m\bar{\sigma}} a^{\dagger}_{m\sigma} a^{\dagger}_{n\bar{\sigma}} a_{n\sigma}) P_{mn} ,$$

where the second term in parenthesis yields zero since $a^{\dagger}_{n\bar{\sigma}}$ attempts to create a $\bar{\sigma}$ spin at site n al-

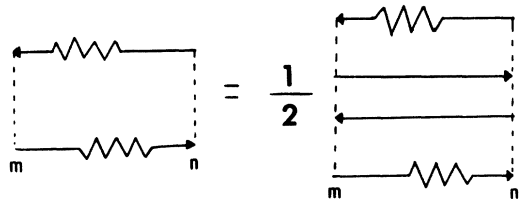

FIG. 10. Theorem A. 2.

though there already is one there owing to the application of P_{nm}.

Employing the Fermion anticommutation relations yields

$$D = \tfrac{1}{2} P_{mn} \sum_{\sigma} (a^{\dagger}_{n\sigma} a_{m\sigma} a^{\dagger}_{m\sigma} a_{n\sigma} + a^{\dagger}_{n\bar{\sigma}} a_{m\bar{\sigma}} a^{\dagger}_{m\sigma} a_{n\sigma}) P_{nm}$$
$$= \tfrac{1}{2} P_{mn} X_{nm} X_{mn} P_{nm} ,$$

thus completing the proof.

For the following theorem we define a *unicyclic* diagram to be a cyclic diagram which has no more than one arrow coming in and one leaving any site.

Theorem A. 3. The diagram obtained on reversing all arrows of a unicyclic diagram D with

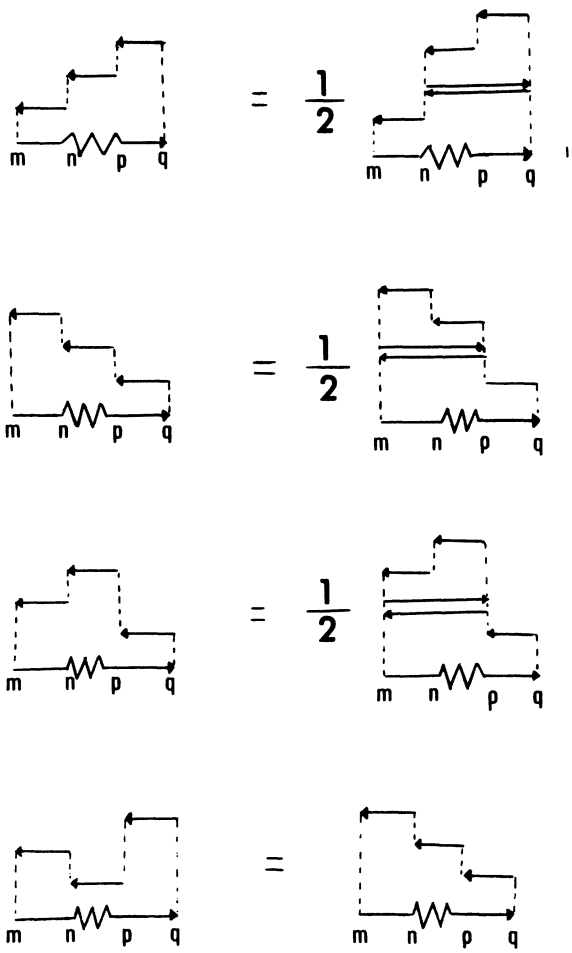

FIG. 11. Diagrams used in the proof of theorem A. 3.

d arrows is equal to $(-1)^d D$.

Proof. The proof is by induction. Equation (A4) establishes it for the two-arrow case, and (A5) along with theorem A. 1 establishes it for the three-arrow case. Assuming that the theorem holds for the $(d-1)$ -arrow case, we seek to prove it for the d-arrow case. For $d \geq 4$ the diagram D must involve at least four sites, say m, n, p, and q. Without loss of generality we take these to be the last four sites involved in D with arrows from n to m, p to n, and q to p. Six orderings for these arrows are possible, four of which are depicted in Fig. 11. The two unlisted orderings differ from the last two diagrams merely by a reordering of X_{mn} and X_{pq}; these two unlisted diagrams are, however, equal to the corresponding listed diagram since X_{mn} and X_{pq} commute. The first three diagrams of Fig. 11 are expressed via theorem A. 2 as a product of two smaller unicyclic diagrams, say D_1 and D_2,

$$D = D_1 D_2 .$$

Since D_1 involves three arrows in each of these cases and D_2 involves $d-1$ arrows, we see that the arrow reversals of D_1 and D_2 are $-D_1$ and $(-1)^{d-1} D_2$. Then, since the arrow reversal of D is simply the product of the arrow reversals of D_1 and D_2, the theorem is obtained for these first three diagrams of Fig. 11. In the fourth diagram of Fig. 11 we obtain

$$D = D_1 - D_2 ,$$

where D_1 is one of the first three types of diagrams and D_2 involves $d-1$ arrows. Noting that the arrow reversal of D is the sum of the arrow reversals of D_1 and D_2 and that D_1 and D_2 satisfy the theorem, the theorem is established for this fourth, and final, type of diagram in Fig. 11.

Corollary. The diagram obtained by turning a unicyclic diagram with d arrows upside down is equal to $(-1)^d D^\dagger$.

Application of these theorems reduces all the more complex linked diagrams to products of the basic two- and three-arrow linked diagrams. Examples of the application of these theorems are found in Appendix C.

APPENDIX B: DOUBLE-COSET FORMULATION

In this appendix we outline an alternate manner in which Hamiltonians such as the Hubbard Hamiltonian may be presented. This alternate formulation leads to the perturbation expansion in terms of products of double cosets of the symmetric group In this formulation, diagrams are evaluated by multiplying double cosets, which sometimes is less tedious.

We first consider a general Schrödinger Hamiltonian H and its representation on the antisymmetrized portion of a space $\mathfrak{V}$ with a basis of normalized product kets

$$|K^0;\ \alpha^0 \gamma^0\rangle \otimes |\sigma\rangle \equiv \left(\prod_m{}^{\cdot}\ |K_m;\ \alpha_m \gamma_m\rangle\right) \otimes |\sigma\rangle . \quad \text{(B1)}$$

Here $|K_m;\ \alpha_m \gamma_m\rangle$ is a spin-free ket for the electrons assigned to site m in the site configuration K_m; also $|K_m;\ \alpha_m \gamma_m\rangle$ transforms as the γ_m row of the α_m irreducible representation for the symmetric group $\mathcal{S}_{(m)}$ of permutations on the spin-free electron indices assigned to that site. The ket $|\sigma\rangle$ is an N-electron spin function. We also make abbreviations

$$\begin{aligned} K^0 &\equiv \prod_m{}^{\cdot}\ K_m , \quad \alpha^0 \equiv \prod_m{}^{\cdot}\ \alpha_m , \\ \gamma^0 &\equiv \prod_m{}^{\cdot}\ \gamma_m \qquad \mathcal{S}^0 \equiv \prod_m{}^{\cdot}\ \mathcal{S}_{(m)} . \end{aligned} \quad \text{(B2)}$$

We identify $\mathcal{S}^0$ as the permutation group which transfers no electrons among sites once they are assigned to sites as in $|K^0;\ \alpha^0 \gamma^0\rangle$. Letting

$$\mathcal{A} \equiv \frac{1}{N!} \sum_{P \in \mathcal{S}_N} (-1)^P P \otimes P \quad \text{(B3)}$$

denote the antisymmetrizer for the total N-electron system, we define the effective Hamiltonian

$$H_{eff} = \sum_{K^0 K^{0'}} \sum_{\alpha^0 \gamma^0} \sum_{\alpha^{0'} \gamma^{0'}} N! \left(\frac{f^{\alpha^0} f^{\alpha^{0'}}}{g^0 g^{0'}}\right)^{1/2} |K^0;\ \alpha^0 \gamma^0\rangle$$

$$\times \langle K^{0'};\ \alpha^{0'} \gamma^{0'}| \otimes \langle K^0;\ \alpha^0 \gamma^0 | \mathcal{A} H\ |K^{0'};\ \alpha^{0'} \gamma^{0'}\rangle , \quad \text{(B4)}$$

where g^0 and $g^{0'}$ are the orders of $\mathcal{S}^0$ and $\mathcal{S}^{0'}$. We note $\langle K^0;\ \alpha^0 \gamma^0 |\mathcal{A} H\ | K^{0'};\ \alpha^{0'} \gamma^{0'}\rangle$ is an operator on spin space. Matrix elements of H_{eff} over basis kets such as (B1) are of the form

$$\begin{aligned} &\langle \sigma\ |\ \langle K^0;\ \alpha^0 \gamma^0\ |\ H_{eff}\ |\ K^{0'};\ \alpha^{0'} \gamma^{0'}\rangle\ |\ \sigma'\rangle \\ &= N! \left(\frac{f^{\alpha^0} f^{\alpha^{0'}}}{g^0 g^{0'}}\right)^{1/2} \langle \sigma\ |\ \langle K^0;\ \alpha^0 \gamma^0\ |\ \mathcal{A} H\ |\ K^{0'};\ \alpha^{0'} \gamma^{0'}\rangle\ |\ \sigma'\rangle \end{aligned} \quad \text{(B5)}$$

if we assume the orthogonality conditions

$$\begin{aligned} &\langle K^0;\ \alpha^0 \gamma^0\ |\ K^{0'};\ \alpha^{0'} \gamma^{0'}\rangle \\ &\qquad = \delta(K^0, K^{0'})\, \delta(\alpha^0, \alpha^{0'})\, \delta(\gamma^0, \gamma^{0'}) . \end{aligned} \quad \text{(B6)}$$

Here we assume (B6), regardless of the number of electrons assigned to the various sites.

We shall employ the double coset decomposition of $\mathcal{S}_N$ with respect to $\mathcal{S}^0$ and $\mathcal{S}^{0'}$ on the left and right,

$$\mathcal{S}_N = \sum_q{}^{\oplus}\ \mathcal{S}^0 G_q\, \mathcal{S}^{0'} . \quad \text{(B7)}$$

Here G_q is a generator of the qth double coset $\mathcal{S}^0 G_q \mathcal{S}^{0'}$, and each element of $\mathcal{S}_N$ is contained in one and only one such double coset. It may be shown[19] that

$$N!\left(\frac{f^{\alpha^0}f^{\alpha^{0\prime}}}{g^0 g^{0\prime}}\right)^{1/2}\langle K^0;\ \alpha^0\gamma^0 \mid \mathcal{A}H \mid K^{0\prime};\ \alpha^{0\prime}\gamma^{0\prime}\rangle$$

$$=\left(\frac{g^0 g^{0\prime}}{f^{\alpha^0}f^{\alpha^{0\prime}}}\right)^{1/2}\sum_q \frac{(-1)^{G_q}}{d_q}$$

$$\times\sum_{S^0 S^{0\prime}}\langle K^0;\ \alpha^0 S^0 \mid G_q H \mid K^{0\prime};\ \alpha^{0\prime} S^{0\prime}\rangle e^{\tilde{\alpha}^0}_{\tilde{\gamma}^0\tilde{s}^0} G_q e^{\tilde{\alpha}^{0\prime}}_{\tilde{s}^{0\prime}\tilde{\gamma}^{0\prime}}\ , \tag{B8}$$

where d_q is the order of the intersection $\mathcal{S}^0 \cap G_q \mathcal{S}^{0\prime} G_q^{-1}$ and $\tilde{\alpha}^0$ denotes the representation of $\mathcal{S}^0$ conjugate to α^0. The group algebraic elements $e^{\tilde{\alpha}^0}_{\tilde{\gamma}^0\tilde{s}^0}$ are matric basis elements with $e^{\tilde{\alpha}^0}_{\tilde{\gamma}^0\tilde{\gamma}^0}$ being a primitive idempotent projecting the symmetry $\tilde{\alpha}^0\tilde{\gamma}^0$ of $\mathcal{S}^0$. Further it may be shown[20] that the double cosets of (B7) are in one-to-one correspondence with the possible patterns in which electrons may be transferred among sites. Thus if G_q transfers D^q_{mn} electrons from site n of $\mathcal{S}^{0\prime}$ to site m of $\mathcal{S}^0$, then the double coset $\mathcal{S}^0 G_q \mathcal{S}^{0\prime}$ is identified[19,21] by a pattern with D^q_{mn} arrows directed from site n to site m.

Substitution of (B8) into (B4) yields an effective Hamiltonian expanded in terms of double cosets. Matrix elements of H_{eff} over a basis of product kets are the same, up to proportionality, as the matrix elements of H over the antisymmetrically projected components of these same product kets. The $N!\,(f^{\alpha^0}f^{\alpha^{0\prime}}/g^0 g^{0\prime})^{1/2}$ factor is introduced in (B4) on account of the normalization of the antisymmetrically projected kets

$$N!\left(\frac{f^{\alpha^0}f^{\alpha^{0\prime}}}{g^0 g^{0\prime}}\right)^{1/2}\langle K^0;\ \alpha^0\gamma^0 \mid \mathcal{A} \mid K^{0\prime};\ \alpha^{0\prime}\gamma^{0\prime}\rangle$$

$$=\delta(\alpha^0,\ \alpha^{0\prime})\,\delta(K^0,\ K^{0\prime})e^{\tilde{\alpha}^0}_{\tilde{\gamma}^0\tilde{\gamma}^{0\prime}}\ , \tag{B9}$$

which results on assuming strong orthogonality between kets on different sites. Diagonalization of H_{eff} on the product basis thus yields the desired energies.

For the Hubbard model we consider only ground states of the various sites with zero, one, or two electrons. The two-electron state is taken as a singlet. In this case, all α^0 are one-dimensional so that the γ^0 index does not occur, and all the K^0 are in one-to-one correspondence with an α^0, so that K^0 may be suppressed. Further, the matrix elements which arise are assumed to be given as

$$\langle \alpha^0 \mid G_q H \mid \alpha^{0\prime}\rangle = \delta(q,0)m_{\alpha^0} I + \delta(q,\rightarrow)T\ . \tag{B10}$$

Here $\delta(q,0)$ is zero unless $q=0$, the identity double coset with no arrows in its diagram; m_{α^0} denotes the number of doubly occupied sites. Also $\delta(q,\rightarrow)$ is zero unless exactly one electron is transferred by G_q from a site in $\mid \alpha^0\rangle$ to a nearest-neighbor site in $\mid \alpha^{0\prime}\rangle$. The effective Hamiltonian for the linear Hubbard case thus becomes

$$H_{eff} = I\sum_{\alpha^0} m_{\alpha^0}\mid \alpha^0\rangle\langle\alpha^0\mid \otimes e^{\tilde{\alpha}^0}$$

$$+T\sum_{\alpha^0,\alpha^{0\prime}}\ \sum_m\ \sum_{n=m\pm1}(-1)^{G_{m\rightarrow n}}[N_m(N_n+1)]^{1/2}$$

$$\times\mid \alpha^0\rangle\langle\alpha^{0\prime}\mid \otimes e^{\tilde{\alpha}^0}\,G_{m\rightarrow n}e^{\tilde{\alpha}^{0\prime}}\ . \tag{B11}$$

Here we have noted that[14]

$$(g^0 g^{0\prime}/d_{m\rightarrow n})^{1/2} = [N_m(N_n+1)]^{1/2}, \tag{B12}$$

with N_m and N_n the numbers of electrons on sites m and n in $\mid \alpha^0\rangle$. Typically we may pick the $G_{m\rightarrow n}$ to be the identity, since $\mid m\rightarrow n\rangle$ has one electron more on site n and one less on site m than does $\mid \alpha^0\rangle$.

In a perturbation expansion of H_{eff} treating the I term as the zero-order Hamiltonian we now identify the diagrams as described in Sec. III as products of double cosets. We illustrate some of these ideas by evaluating a couple of basic diagrams. We denote the zero-order choice for α^0 by 0, and assign electron m to site m in $\mid 0\rangle$. A configuration differing from $\mid 0\rangle$ only in that an electron m is transferred to site n is denoted $\mid m\rightarrow n\rangle$. We note that $e^0 = 1$ and that $e^{m\rightarrow n}$ is a singlet projector for electrons m and n. For the simple two-arrow diagram of Fig. 2 we thus obtain

$$(1\cdot 2)^{1/2}(2\cdot 1)^{1/2}\mid 0\rangle\langle m\rightarrow n \mid m\rightarrow n\rangle\langle 0\mid$$

$$\otimes e^0 e^{m\rightarrow n}e^{m\rightarrow n}e^{\tilde{0}} = 2\mid 0\rangle\langle 0\mid\otimes e^{m\rightarrow n}$$

$$= \mid 0\rangle\langle 0\mid\otimes\{1-(mn)\}\ , \tag{B13}$$

in agreement with (A4). Similarly we may treat the three-arrow diagram of Fig. 9,

$$(1\cdot 2)^{1/2}(2\cdot 2)^{1/2}(2\cdot 1)^{1/2}\mid 0\rangle\langle m\rightarrow p \mid (m\rightarrow n)\rightarrow p\rangle$$

$$\times\langle m\rightarrow n \mid m\rightarrow n\rangle\langle 0\mid$$

$$\otimes e^0 e^{m\rightarrow p}e^{(m\rightarrow n)\rightarrow p}e^{m\rightarrow n}e^0$$

$$= 4\mid 0\rangle\langle 0\mid\otimes e^{m\rightarrow p}e^{m\rightarrow n}$$

$$= \mid 0\rangle\langle 0\mid\otimes\{1-(mp)\}\{1-(mn)\}$$

$$= \mid 0\rangle\langle 0\mid\otimes\{1-(mp)-(mn)-(mnp)\}$$

$$= \mid 0\rangle\langle 0\mid\otimes\{(np)-(mpn)\}, \tag{B14}$$

where $(m\rightarrow n)\rightarrow p$ is the configuration differing from $m\rightarrow n$ only in having electron m transferred from site n to site p. The result (B14) checks with (A5), although the procedure here is less tedious.

APPENDIX C: DIAGRAM EVALUATIONS

In this appendix we illustrate the evaluation of several types of diagrams which appear in the fourth- and sixth-order expansions. First we consider the cyclic four-arrow diagrams appearing

in $\mathfrak{L}(1,1,1)$. Using theorem A. 2 on the diagrammatic representation of $\mathfrak{L}(1,1,1)$ yields the result of Fig. 4. Now since the upper and lower three-arrow diagrams on the right-hand side of the equation in Fig. 3 are evaluated using Eq. (A5) along with theorems A. 1 and A. 3, we obtain

$$\begin{aligned}(\text{Fig. } 3) = \frac{1}{2}\sum_n \{&[(n+1,n+2)-(n,n+1,n+2)][(n+1,n+2)-(n,n+2,n+1)]+[(n,n+2,n+1)-(n,n+1)]\\ &\times[(n,n+1,n+2)-(n,n+1)]+[(n+1,n+2)-(n,n+1,n+2)][(n,n+1,n+2)-(n,n+1)]\\ &+[(n,n+2,n+1)-(n,n+1)][(n+1,n+2)-(n,n+2,n+1)]\}\\ &= 4A_1 - A_2. \end{aligned} \tag{C1}$$

Here we have multiplied out the permutations, used Eq. (A3), and collected terms.

Next we wish to evaluate the linked portion of (1, 0, 1), as given in Fig. 4:

$$\begin{aligned}(\text{Fig. } 4) = \sum_n \{&[1-(n+1,n+2)][1-(n,n+1)]\\ &+[1-(n,n+1)]^2+[1-(n,n+1)][1-(n+1,n+2)]\}\\ &= 4A_1 - A_2. \end{aligned} \tag{C2}$$

Here we have again used Eq. (A3).

On using similar techniques, the sixth-order diagrams of Fig. 5, as appear in $\mathfrak{L}(1,1,1,1,1)$, become

$$\mathfrak{L}(\text{type } a) = 48A_1 - 12A_2 - 2B_1 - 2B_2 + 2B_3,$$

$$\mathfrak{L}(\text{type } b) + \mathfrak{L}(\text{type } d) = 168A_1 - 48A_2 + 24A_3 - 72B_1 + 24B_2 - 24B_3, \tag{C3}$$

$$\mathfrak{L}(\text{type } f) = 2A_1 - B_1.$$

Substitution of (C3) into (4. 5) yields (4. 6). If we identify the first five diagrams of Fig. 6 as D_1, D_2, D_3, D_4 and D_5, then the present methods yield

$$D_1 + D_2 + D_3 + D_4 + D_1^\dagger + D_2^\dagger + D_3^\dagger + D_4^\dagger = 46A_1 - 12A_2 + 2A_3 - 8B_1 \tag{C4}$$

and

$$\tfrac{1}{2}(D_5 + D_5^\dagger) = 12A_1 - 8A_2 + 4A_3 - 4B_1 + 4B_2 - 4B_3. \tag{C5}$$

Addition of (C4) and (C5) then multiplication by four yields (4. 7). Addition of (C4) and $\frac{1}{2}$ of (C5) followed by multiplication by four yields (4. 8). Similar techniques may be used to evaluate (4. 9).

†Supported by the Robert A. Welch Foundation, Houston, Texas and the National Science Foundation, Washington, D. C.

*NSF Trainee.

[1]J. Hubbard, Proc. R. Soc. A 276, 238 (1963); Proc. R. Soc. A 277, 237 (1963); Proc. R. Soc. A 281, 401 (1964).

[2](a) M. C. Gutzwiller, Phys. Rev. Lett. 10, 159 (1963). (b) J. Kanamori, Prog. Theor. Phys. 30, 275 (1963).

[3](a) P. J. Strebel and Z. G. Soos, J. Chem. Phys. 53, 4077 (1970). (b) D. J. Klein and Z. G. Soos, Mol. Phys. 20, 1013 (1971). (c) Z. G. Soos and D. J. Klein, J. Chem. Phys. 55, 3284 (1971). (d) Z. G. Soos and A. J. Silverstein, Mol. Phys. 23, 775 (1972).

[4](a) A. J. Epstein, S. Etemad, A. F. Garito, and A. J. Heeger, Phys. Rev. B 5, 952 (1972). (b) A. N. Bloch, R. B. Weisman, and C. M. Verma, Phys. Rev. Lett. 28, 753 (1972). (c) E. Ehrenfreund, S. Etemad, L. B. Coleman, E. F. Rybaczewski, A. F. Garito, and A. J. Heeger, Phys. Rev. Lett. 29, 269 (1972).

[5]J. des Cloizeaux, Nucl. Phys. 20, 321 (1960).

[6]D. J. Klein (unpublished).

[7]L. N. Buleavski, Zh. Eksp. Teor. Fiz. 51, 230 (1966) [JETP 24, 154 (1967)].

[8]H. Primas, Helv. Phys. Acta 34, 331 (1961).

[9]P. W. Anderson, Phys. Rev. 115, 2 (1959).

[10](a) H. Shiba and P. A. Pincus, Phys. Rev. B 5, 1966 (1972). (b) K. -H. Heinig and J. Monecke, Phys. Status Solidi 49, K139, K141 (1972). (c) D. Cabib and T. A. Kaplan, Phys. Rev. B 7, 2199 (1973).

[11]J. C. Bonner and M. E. Fisher, Phys. Rev. 135, A640 (1964).

[12]Functional-integral methods: (a) S. Q. Wang, W. E. Evenson, and J. R. Schrieffer, Phys. Rev. Lett. 23, 92 (1969). (b) M. Cyriot, Phys. Rev. Lett. 25, 871 (1971). (c) W. E. Evenson, J. R. Schrieffer, and S. Q. Wang, J. Appl. Phys. 41, 1199 (1970).

[13]Random-phase-approximation and Green's function methods: (a) D. R. Penn, Phys. Rev. 142, 350 (1966). (b) W. Langer, M. Plischke, and D. C. Mattis, Phys. Rev. Lett. 23, 1448 (1969). (c) R. A. Bari and R. V. Lange, Phys. Lett. 30A, 418 (1969). (d) L. M. Roth, Phys. Rev. 184, 451 (1969); Phys. Rev. 186, 428 (1969). (e) T. Arai, Phys. Rev. B 4, 216 (1971).

[14]High-temperature-series expansions: L. N. Buleavski and D. I. Khomskii, Phys. Lett. 41A, 257 (1972).

[15](a) F. Y. Wu and E. H. Lieb, Phys. Rev. Lett. 20, 1445 (1968). (b) M. Takahashi, Prog. Theor. Phys. 42, 1098 (1969); Prog. Theor. Phys. 43, 1619 (1970). (c) A. A. Ovchinnikov, Zh. Eksp. Teor. Fiz. 57, 2137 (1969) [JETP 30, 1160 (1970)].

[16]Kato, Prog. Theor. Phys. 4, 154 (1949).

[17](a) P. O. Löwdin, J. Chem. Phys. 18, 365 (1950). (b) P. O. Löwdin, Adv. Phys. 5, 1 (1956).

[18]M. Moshinsky, *Group Theory and the Many-Body Problem* (Gordon and Breach, New York, 1968).

[19]F. A. Matsen, D. J. Klein, and D. C. Foyt, J. Phys. Chem. 75, 1866 (1971).
[20](a) P. Kramer and T. H. Seligman, Nucl. Phys. A 136, 545 (1969); Nucl. Phys. A 186, 49 (1972). (b) B. R. Junker and D. J. Klein, J. Chem. Phys. 55, 5533 (1971).
[21]C. Herring, *Magnetism* 2*B*, edited by G. T. Rado and H. Suhl (Academic, New York, 1963), p. 1.